Kinetic Energy Concentration of a Relativistic Bremsstrahlung Electron

Mert Yücemöz[1]

[1]University of Bath

Key Points:

- A new formula was developed to predict the change in kinetic energy distribution within a bremsstrahlung electron.
- The energy is concentrated at the outer region of the bremsstrahlung electron, opposite to the direction of centripetal acceleration.
- Shrinking radiation lobe due to the bremsstrahlung asymmetry goes into increasing local energy concentration within the electron.

Corresponding author: Mert Yucemoz, m.yucemoz@bath.ac.uk

Abstract

Terrestrial Gamma-ray Flashes exhibit slopes of ionizing radiation associated with bremsstrahlung. Bremsstrahlung has a continuous spectrum of radiation from radio waves to ionizing radiation. The Poynting vector of the emitted radiation, i.e., the radiation pattern around a single particle under the external lightning electric field during interaction with other particles or atoms, is not quite well known. The overall radiation pattern arises from the combination of radiation of parallel and perpendicular motions of a particle caused by the acceleration from the lightning electric field and the bremsstrahlung. The calculations and displays of radiation patterns are generally limited to a low-frequency approximation for radio waves and separate parallel and perpendicular motions. Here we report the radiation patterns of combined parallel and perpendicular motions from accelerated relativistic particles at low and high frequencies of the bremsstrahlung process with an external lightning electric field. The primary outcome is that radiation patterns have four relative maxima with two forward peaking and two backward peaking lobes. The asymmetry of the radiation pattern, i.e., the different intensities of forward and backward peaking lobes, are caused by the Doppler effect. A novel outcome is that bremsstrahlung has an asymmetry of the four maxima around the velocity vector caused by the curvature of the particle's trajectory as it emits radiation. In addition, change in kinetic energy of bremsstrahlung electron and shrinking radiation lobe due to bremsstrahlung asymmetry were found to increase electron's energy concentration towards the outer regions of the curved trajectory. This mathematical modeling helps to better understand the physical processes of a single particle's radiation pattern, which might assist the interpretation of observations with networks of radio receivers and arrays of γ-ray detectors.

1 Introduction

It was recently suggested that high-frequency radiation emissions observed in the atmosphere could originate from muons interacting with electric fields inside thunderclouds. This novel idea is based on a reduction of the muon detection during thunderstorm occurrences by the ground based telescope GRAPES-3 located in Ooty, India (Hariharan et al., 2019). Gamma-Ray Bursts (GRBs) are commonly thought to result from the interaction of neutron stars in outer space or comet collisions. GRBs emit photons in the energy range from keV to MeV that last ∼10 seconds. However, a ∼90 minute long GRB was detected with photon energies ∼18 GeV (Hurley et al., 1994). When Terrestrial Gamma-Ray Flashes (TGFs) were first observed by detectors of the Compton Gamma Ray Observatory (CGRO) (Fishman et al., 1994), their association with bremsstrahlung was demonstrated by the observation of the characteristic slopes of ionizing radiation (Dwyer et al., 2012a), supported by Monte Carlo simulations that included the bremsstrahlung process (Dwyer, 2007). Another example of bremsstrahlung associated with lightning discharges is the detection of ultra-low frequency (ULF) and very low frequency (VLF) radio emissions of the same electrons that are also responsible for emitting terrestrial gamma-ray flashes (Connaughton et al., 2013). TGFs are associated with low-frequency radio emissions, and these observations were used to identify their source altitude (Pu et al., 2019; Cummer et al., 2014). The source altitude was located to lie between two charged cloud layers in a thunderstorm. All the above discoveries offer experimental evidence for the continuous radiation spectrum of bremsstrahlung to occur. Relativistic runaway electrons are the source of high-frequency X- and γ-ray emissions observed in the upper troposphere at altitudes from ∼12-14 km height (Celestin, 2016). High energy relativistic electrons have a larger mean free path such that they can attain larger velocities until they collide with an atom or molecule in the atmosphere. As these electrons are capable of reaching large velocities, they can emit ionizing radiation through the bremsstrahlung process. Low energy electrons are much more likely to collide with atmospheric atoms or molecules, leading to an increase in the number of free electrons in the atmosphere (Celestin, 2016). Another working hypothesis is that bremsstrahlung radiation is emitted by thermal runaway electrons accelerated by intra-cloud lightning leader tips (Xu

et al., 2015). Bremsstrahlung has a continuous electromagnetic spectrum. Low-frequency radio and optical emissions could also be due to fluorescence, where high-frequency TGFs are absorbed by air molecules (Xu et al., 2015). Numerical Monte Carlo simulations demonstrated the significance of the bremsstrahlung process as the primary process behind high-frequency emissions (Dwyer et al., 2012b). Bremsstrahlung electrons emit radiation in forward peaking radiation patterns with an angle that scales with the inverse of the Lorentz factor of the relativistic electrons (Koch & Motz, 1959).

Asymmetric signal of γ-ray bursts measured by the Gamma-Ray Burst Monitor on the Fermi Gamma-ray Space Telescope reveal the lightning leader charge structure. Asymmetric γ-ray pulses indicate the lightning leader charge flux, which exhibits a fast rise and slow decay of the leader tip electric field (Foley et al., 2014). The asymmetries in γ-ray pulses are thought to be caused by Compton scattering (Xu et al., 2019). The rise to decay time ratio of single γ-ray pulses was measured to be approximately 0.67 (Nemiroff et al., 1994). Data from the Burst and Transient Source Experiment (BATSE) reveals two different types of spectra of γ-ray bursts known as bright and dim GRBs. It was found that dim GRBs have less photon energy than bright GRBs (Norris et al., 1994). It was observed that as time passes, overall γ-ray photons transit from bright to dim photons as a photon bunch due to a time delay of approximately 100 μs between the peaks arising from hard and soft photons (Grefenstette et al., 2008).

Experimental measurements of ionizing radiation and optical emissions by the Atmosphere Space Interactions Monitor (ASIM) on the International Space Station recently reported the detection of 217 TGFs from June 2, 2018, to April 1, 2019 (Østgaard et al., 2019), some associated with radio emissions from charged particles that are observed on the ground. All these measurements reveal the properties of γ-ray bursts. After the combination of the measurements from ground-based radio receivers and spacecraft, it was found that TGFs are produced at the very beginning of the lightning discharge process. It is well known that the observed γ-rays originate from the bremsstrahlung process (Xu et al., 2015). There are approximately $\sim 10^{17}$–10^{19} Gamma-ray bursts emitted during the bremsstrahlung process. It is well known that the initially emitted ionizing radiation is not the same in terms of energy and direction compared to the radiation measured by sensors. This difference is because the emitted radiation loses energy by backscattering and interacting with other air molecules. The interaction causes an ionization and releases more electrons, which can explain why $10^{17} - 10^{19}$ γ-rays are emitted (Dwyer, 2008). Another theory explains γ-ray bursts to originate from the large electric fields of leader tip streamers producing $\sim 10^{12}$ electrons which then increase the number of electrons within the relativistic runaway electron avalanche (RREA) process that emits γ-ray photons (Babich et al., 2014, 2015; Moss et al., 2006; Chanrion & Neubert, 2010; Celestin & Pasko, 2011; Skeltved et al., 2017).

This contribution reports the modeling of an asymmetric forward peaking radiation pattern and an asymmetric backward peaking radiation pattern of a single particle bremsstrahlung process. The asymmetry occurs around the horizontal axis parallel to the direction of motion of the charged particle, and it is unique to the bremsstrahlung process as the particle continuously follows a curved trajectory of an anticlockwise rotation. Radiation patterns are calculated for both relativistic and non-relativistic velocities. The main asymmetry with four radiation peaks is unique to the bremsstrahlung process and occurs when the particle radiation transits from a dipole towards forward and backward peaking radiation patterns. In addition, bremsstrahlung asymmetry, R, was found to shrink the radiation lobe in one direction, which goes into increasing electron's internal energy at that region (outer part of the electron). Moreover, bremsstrahlung electron's internal energy also increases in outer region as a result of acceleration process (change in kinetic energy) in a curved trajectory. This can be visualised as standing people in the bus. As the bus gets into the bend, people standing starts to fall over to the outer side of the bus.

1.1 Aims & Objectives

This contribution aims to understand and predict the effects of the bremsstrahlung asymmetry parameter, R on particle's (electron) internal energy concentration. Moreover, to understand how a change in a particle's kinetic energy during the acceleration process in a curved trajectory affects the particle's internal energy distribution. To model a particle's internal energy distribution, the main quantity used is the electron's rest mass rather than the electron's radius which is true for classical mechanics. By using the Dirac delta function with the electron's rest mass, along with bremsstrahlung asymmetry and the kinetic energy equation, the electron's internal energy distribution is modeled.

2 Particle Position Vector

Starting with defining a curved path for a bremsstrahlung electron.

The position vector is formulated for a particle trajectory that is an anti-clockwise rotating spiral as a function of the retarded time characteristic for bremsstrahlung radiation.

The position vector in equation 1 defines a spiral trajectory for an incoming particle, i.e., an electron, induced by the Coulomb force of the target particle that causes the emission of bremsstrahlung radiation (Figure 2a). The spiral trajectory in Figure 2a and mathematically defined in equation 1 is realistic even though the mean free path is quite short, e.g., nm-μm in the atmosphere with a high recombination rate. For example, a circle with a radius of 1 m could also have a radius of 2 μm, depending on the medium and the recombination rate. It is still a circle but a scaled microscopic version of the initial macroscopic circle. Preserving geometry at different scales is also true in the formulated spiral trajectory (Eq.1). The decision on a specific particle trajectory considers the ratio of particle size to a curved trajectory radius. If the particle size is larger than the curvature radius, the particle trajectory is approximately a straight line. Therefore, a spiral particle trajectory is realistic because an electron has a size of $< 2.8 \times 10^{-19}$ m as measured by the Hadron-Electron Ring Accelerator (HERA) in Hamburg, Germany at the Deutsches Electronen Synchrotron (DESY) facility (Bourilkov, 2000).

$$r(t) = \frac{(t^R)^2 b^R (\omega^{'})^R cos(\theta_{n,r(t)})^R c}{\tau^{2R} c^R \omega^{'} cos(\theta_{n,r(t)})} - \frac{at}{\tau}, \tag{1}$$

where $r(t)$ is the position vector as a function of time t in s, R is the dimensionless bremsstrahlung asymmetry index, τ is the mean free time in s. Also, $\omega^{'}$ is the angular frequency of the emitted electromagnetic wave in the frame of reference of the particle in rads/s, c is the speed of light, $\theta_{n,r(t)}$ is the angle between the emitted radiation unit vector n and the particle's position vector. The time range of the position vector is $-\infty < t < +\infty$. In addition, the factor b in m describes the interaction distance between the incoming particle and the target particle, which is the radius of the time-dependent position vector. The radius of the position vector is directly proportional to the parameter b. This radius of curvature is related to the mean free path because the curvature increases with time, contributing to the overall arc length, i.e., the mean free path of the accelerated particle. In other words, $b \propto \lambda_{v/c}$, where $\lambda_{v/c}$ is the mean free path of a particle at the velocity v which is given as a percentage of the speed of light v/c. The factor a in m is an arbitrary adjustment parameter. It is introduced to correct the radius of the curvature of a particle during the bremsstrahlung process. This correction is required because the trajectory of a relativistic particle shrinks in size over time, and a propagation close to the speed of light introduces significant changes in the mean free path. Finally, equation 1 is a function of time t. Hence, the particle will only cover some segment, or arc length, of the spiral, or the complete arc length of a particle's spiral trajectory when $t = \tau$.

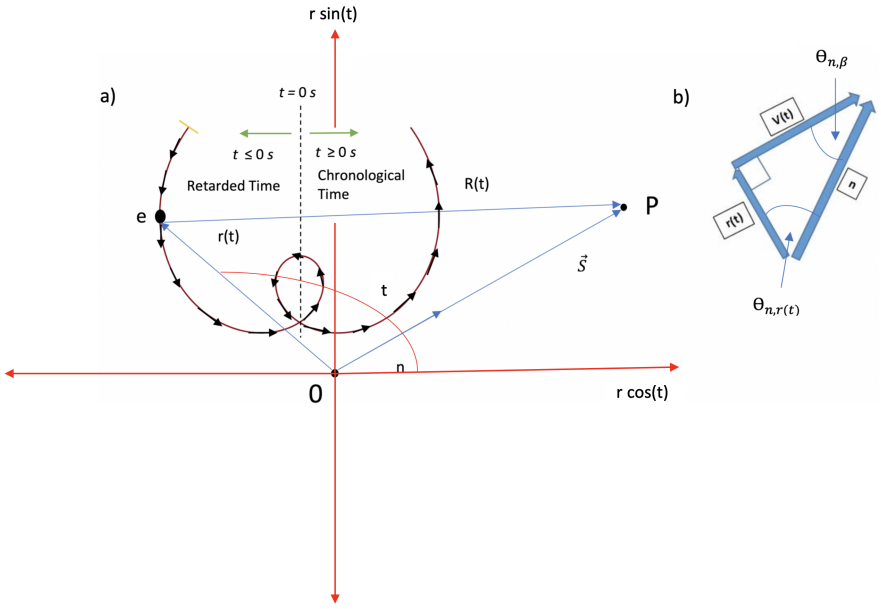

Figure 1. a) Trajectory of the bremsstrahlung electrons given by equation (1) in a polar co-ordinate system and radiation emissions by the change in velocity over time by a Coulomb force of other charges. O represents the target particle that defines the electron's spiral trajectory due to the Coulomb force (equation 1). The electron acceleration and corresponding velocity vectors are displayed with black arrows and are tangential to the spiral trajectory (red line) and perpendicular to the position vector $r(t)$. $R(t_r)$ is the distance between the accelerated electron and the observer, which is a function of both retarded and chronological time (t_r, t). P is the position of an observer. $\vec{S}$ is the Poynting vector, or radiant energy flux, which determines the direction of the energy flow per area of an emitted electromagnetic wave. The dimensionless unit vector n points in the direction of the Poynting vector $\vec{S}$. b) The position vector $r(t)$, velocity vector $v(t)$ and the unit radiation vector n form a rectangular triangle.

3 Change in Energy within a Single Bremsstrahlung Electron

This section looks at the change in kinetic energy within a bremsstrahlung electron as it accelerates on a curved trajectory. As the electron is a quantum particle, the density of an electron is written in terms of just the electron's rest mass and angle defining the surrounding of an electron. In addition, the use of electron radius is omitted. The density of an electron is written using the Dirac delta function multiplied with electron rest mass, m_o.

$$\frac{dKE}{d\theta_{n,\beta}} = 2c^2 m_o \frac{1}{0.1\sqrt{\pi}} \frac{d\gamma}{dt} e^{-(\frac{\theta_{n,\beta}}{0.1})^2} \tag{2}$$

Where, "KE' stands for kinetic energy and $d\gamma$ is the Lorentz factor. The time derivative of Lorentz factor, $\frac{d\gamma}{dt}$ is $\frac{v}{c^2}(1-\frac{v^2}{c^2})^{-3/2}\frac{dv}{dt}$. In addition, $\frac{dv}{dt}$ is the second order time derivative of the equation 1. Multiplication with two in equation 2, is because there are two angles in three dimensional co-ordinate system (Spherical). Under the assumption of uniformity in all directions, mass of the electron can be proven by integrating Dirac delta function $\frac{1}{0.1\sqrt{\pi}} e^{-(\frac{\theta_{n,\beta}}{0.1})^2}$ over just one angle and by multiplying with factor two.

$$\frac{dr}{dt} = \frac{b^R(\omega^{'})^R cos(\theta_{n,r(t)})^R c}{c^R \omega^{'} \tau^{2R} cos(\theta_{n,r(t)})} \left[2Rt^{2R-1} \right] - \frac{a}{\tau} \tag{3}$$

and acceleration is,

$$\frac{dv}{dt} = \frac{b^R(\omega^{'})^R cos(\theta_{n,r(t)})^R c}{c^R \omega^{'} \tau^{2R} cos(\theta_{n,r(t)})} \left[(4R^2 - 2R)t^{2R-2} \right] \tag{4}$$

4 Results

This section presents predictions of equation 2, describing the internal energy concentration of a relativistic bremsstrahlung electron due to change in kinetic energy on a curved trajectory and the shrinking lobe of the bremsstrahlung asymmetry, R.

Figure 2 shows how a change in kinetic energy of a particle as it accelerates on a curved trajectory goes into increasing the particle's internal energy. This increase in particle's internal energy is also accompanied by the bremsstrahlung asymmetry, R which is also present as a result of the curved trajectory of the particle.

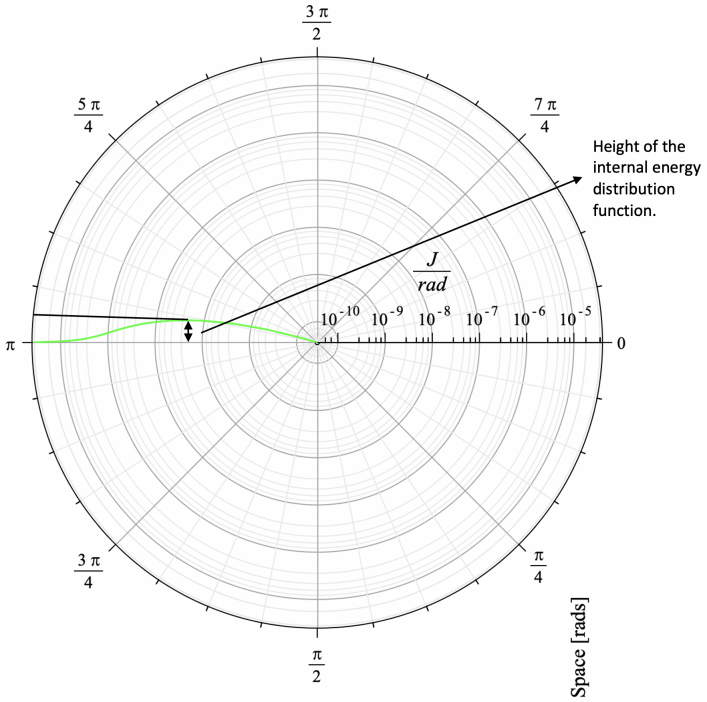

Figure 2. The height of the internal energy distribution function indicates the level of curvature (radius of curvature) and it is indirectly related to the bremsstrahlung asymmetry parameter, R. When a particle goes through a sharp curvature, R increases. However, the height of the function in the plot decreases. This means energy is localizing at a much narrower region. This can be linked to standing people inside a bus that goes through a bend. Sharper the bend, people will be squeezed together at a much narrower space towards the outer side of the bend. The horizontal axis represents the energy gained by a particle through the acceleration process and distribution within the particle. The angle represents the space around the particle.

The fractions presented in figure 3 correspond to the fractions presented in figure 5. The bremsstrahlung asymmetry, R-value represents the sharpness of the curved trajectory. Increasing bremsstrahlung asymmetry, R-value means decreasing radius of curvature. As the particle approaches the minimum of the radius curvature along the curved path, the particle's internal energy distribution converges to a single direction and a narrower region. This effect is presented in figure 3 with different colors of kinetic energy distributions, each corresponding to a single bremsstrahlung asymmetry, R-value. In addition, the decreasing height of the plotted curves with increasing asymmetry displays the convergence of the scalar energy field over a narrower region. Therefore, as the particle rotates in an anti-clockwise direction, the internal scalar energy field concentrates towards the outer part of the electron (figure 4).

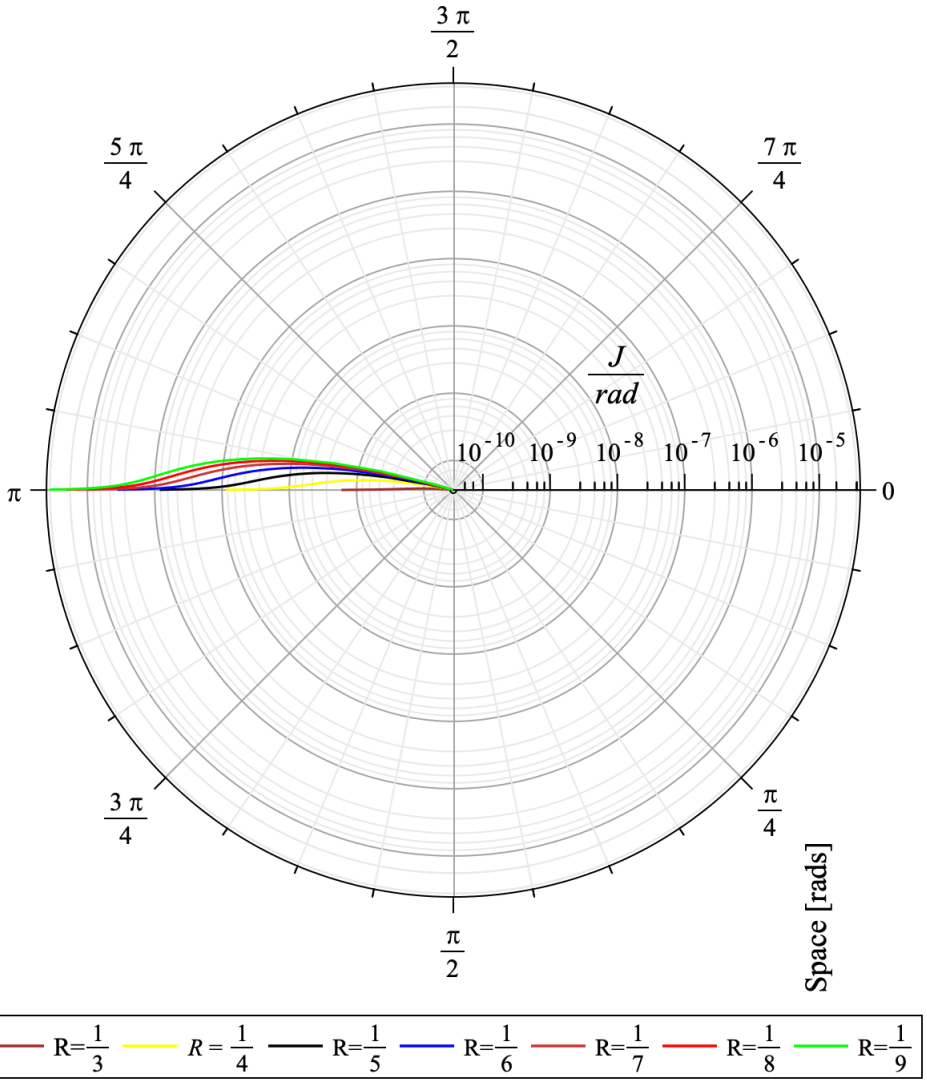

Figure 3. 0 radians is the region of the electron that faces towards the centre of the curved trajectory. In addition, π radians is the region of electron facing outside of the curved trajectory.

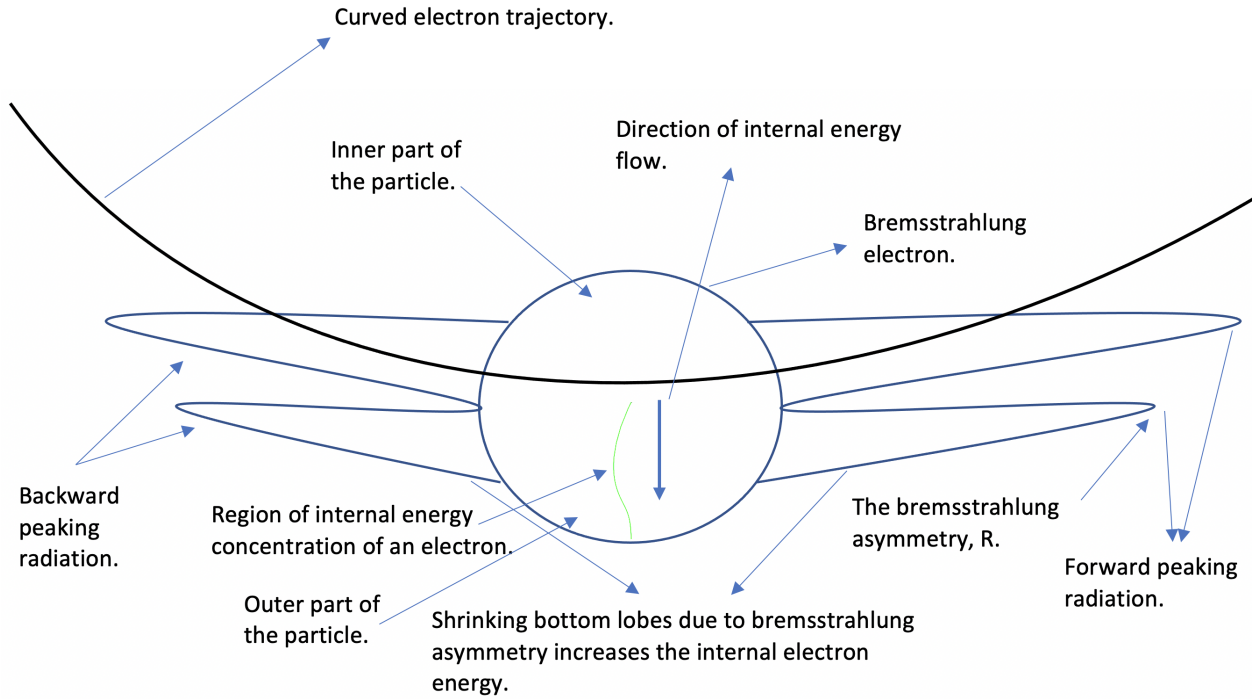

Figure 4. This figure displays location of internal energy concentration of the bremsstrahlung electron due to bremsstrahlung asymmetry and the curved trajectory.

Unlike many of the other radiation emission processes of charged particles (i.e., from linear acceleration or crossing the boundary between two different dielectric media), the bremsstrahlung process affects the shape of the emitted radiation. This bremsstrahlung effect causes an asymmetry of the emitted radiation about the particle's velocity vector or, in other terms, the direction of motion. To understand this effect, we can compare an electron to a car that travels in the dark with the headlight turned on. The headlights are the emitted electromagnetic radiation by the car. When the car gets into the bend, like the bremsstrahlung process of an electron, an observer outside the car can immediately tell the radiation shape of the headlight would be asymmetric by looking at the reflections on the road compared to the case when the car follows a straight path. This novel effect is clearly shown in supporting information in the Figure S1, which displays a real-life example of visible asymmetry of the car headlights (electromagnetic radiation) on a bend.

Figure 5 displays the effects of the bremsstrahlung radiation asymmetry control quantity R. The bremsstrahlung asymmetry R depends on the radius of the curvature of the incoming particle trajectory undergoing the bremsstrahlung process. In addition, the bremsstrahlung asymmetry R increases as the radius of curvature of the bremsstrahlung trajectory decreases.

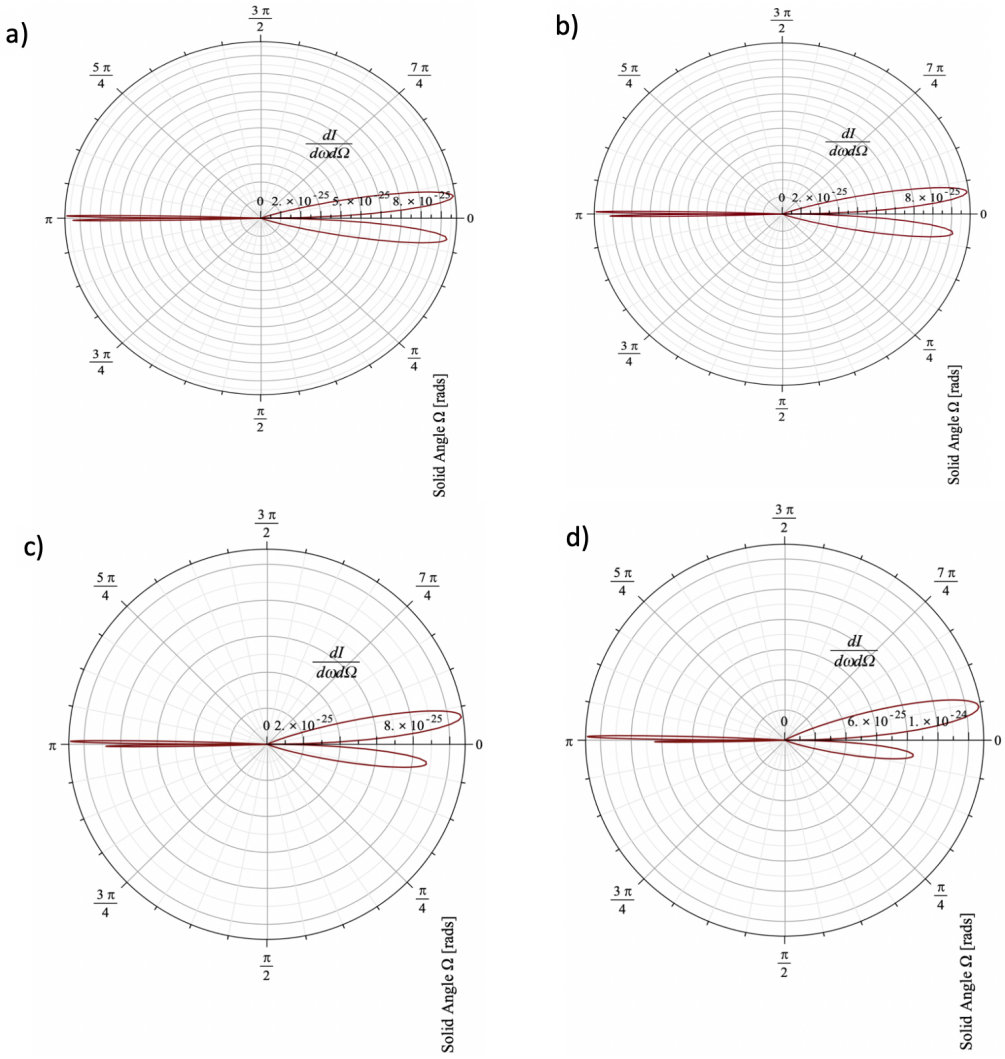

Figure 5. Bremsstrahlung Asymmetry Quantity R with different values. a) $R = \frac{1}{9}$, b) $R = \frac{1}{6}$, c) $R = \frac{1}{4}$, d) $R = \frac{1}{3}$

Acknowledgments

I would like to thank my supervisor Dr.Martin Füllekrug for all the support. My family for their support and good wishes. EPSRC and MetOffice sponsor my PhD project under contract numbers EG-EE1239 and EG-EE1077.

References

Babich, L. P., Bochkov, E. I., & Kutsyk, I. M. (2014). Mechanism of generation of runaway electrons in a lightning leader. *JETP Letters*, *99*(7), 386–390. Retrieved from `https://doi.org/10.1134/S0021364014070029` doi: 10.1134/S0021364014070029

Babich, L. P., Bochkov, E. I., Kutsyk, I. M., Neubert, T., & Chanrion, O. (2015). A model for electric field enhancement in lightning leader tips to levels allowing X-ray and γ ray emissions. *Journal of Geophysical Research: Space Physics*, *120*(6), 5087-5100. Retrieved from `https://agupubs.onlinelibrary.wiley.com/doi/abs/10.1002/2014JA020923` doi: 10.1002/2014JA020923

Bourilkov, D. (2000, Sep). Search for tev strings and new phenomena in bhabha scattering at cern lep2. *Phys. Rev. D*, *62*, 076005. Retrieved from https://link.aps.org/doi/10.1103/PhysRevD.62.076005 doi: 10.1103/PhysRevD.62.076005

Celestin, S. (2016, December). Electron acceleration mechanisms in thunderstorms. *arXiv*, 1-6. doi: arXiv:1701.00105[astro-ph.HE]

Celestin, S., & Pasko, V. P. (2011). Energy and fluxes of thermal runaway electrons produced by exponential growth of streamers during the stepping of lightning leaders and in transient luminous events. *Journal of Geophysical Research: Space Physics*, *116*(A3). Retrieved from https://agupubs.onlinelibrary.wiley.com/doi/abs/10.1029/2010JA016260 doi: 10.1029/2010JA016260

Chanrion, O., & Neubert, T. (2010). Production of runaway electrons by negative streamer discharges. *Journal of Geophysical Research: Space Physics*, *115*(A6), 1-10. Retrieved from https://agupubs.onlinelibrary.wiley.com/doi/abs/10.1029/2009JA014774 doi: 10.1029/2009JA014774

Connaughton, V., Briggs, M. S., Xiong, S., Dwyer, J. R., Hutchins, M. L., Grove, J. E., ... Wilson-Hodge, C. (2013, May). Radio signals from electron beams in terrestrial gamma ray flashes. *Journal of Geophysical Research: Space Physics*, *118*(5), 2313-2320. Retrieved from https://agupubs.onlinelibrary.wiley.com/doi/abs/10.1029/2012JA018288 doi: 10.1029/2012JA018288

Cummer, S. A., Briggs, M. S., Dwyer, J. R., Xiong, S., Connaughton, V., Fishman, G. J., ... Solanki, R. (2014, December). The source altitude, electric current, and intrinsic brightness of terrestrial gamma ray flashes. *Geophysical Research Letters*, *41*(23), 8586-8593. Retrieved from https://agupubs.onlinelibrary.wiley.com/doi/abs/10.1002/2014GL062196 doi: 10.1002/2014GL062196

Dwyer, J. R. (2007). Relativistic breakdown in planetary atmospheres. *Physics of Plasmas*, *14*(4), 042901. Retrieved from https://doi.org/10.1063/1.2709652 doi: 10.1063/1.2709652

Dwyer, J. R. (2008). Source mechanisms of terrestrial gamma-ray flashes. *Journal of Geophysical Research: Atmospheres*, *113*(D10), 1-12. Retrieved from https://agupubs.onlinelibrary.wiley.com/doi/abs/10.1029/2007JD009248 doi: 10.1029/2007JD009248

Dwyer, J. R., Smith, D. M., & Cummer, S. A. (2012a). High-energy atmospheric physics: Terrestrial gamma-ray flashes and related phenomena. *Space Science Reviews*, *173*(1), 133–196. Retrieved from https://doi.org/10.1007/s11214-012-9894-0 doi: 10.1007/s11214-012-9894-0

Dwyer, J. R., Smith, D. M., & Cummer, S. A. (2012b, June). High-Energy Atmospheric Physics: Terrestrial Gamma-Ray Flashes and Related Phenomena. *Space Science Reviews*, *173*(1), 133–196. Retrieved from https://doi.org/10.1007/s11214-012-9894-0 doi: 10.1007/s11214-012-9894-0

Fishman, G. J., Bhat, P. N., Mallozzi, R., Horack, J. M., Koshut, T., Kouveliotou, C., ... Christian, H. J. (1994). Discovery of intense gamma-ray flashes of atmospheric origin. *Science*, *264*(5163), 1313–1316. Retrieved from https://science.sciencemag.org/content/264/5163/1313 doi: 10.1126/science.264.5163.1313

Foley, S., Fitzpatrick, G., Briggs, M. S., Connaughton, V., Tierney, D., McBreen, S., ... Wilson-Hodge, C. (2014, June). Pulse properties of terrestrial gamma-ray flashes detected by the Fermi Gamma-Ray Burst Monitor. *Journal of Geophysical Research: Space Physics*, *119*(7), 5931-5942. Retrieved from https://agupubs.onlinelibrary.wiley.com/doi/abs/10.1002/2014JA019805 doi: 10.1002/2014JA019805

Grefenstette, B. W., Smith, D. M., Dwyer, J. R., & Fishman, G. J. (2008, March). Time evolution of terrestrial gamma ray flashes. *Geophysical Research Letters*,

35(6), 1-5. Retrieved from https://agupubs.onlinelibrary.wiley.com/doi/abs/10.1029/2007GL032922 doi: 10.1029/2007GL032922

Hariharan, B., Chandra, A., Dugad, S. R., Gupta, S. K., Jagadeesan, P., Jain, A., ... Tanaka, K. (2019, Mar). Measurement of the electrical properties of a thundercloud through muon imaging by the grapes-3 experiment. *Phys. Rev. Lett.*, *122*, 105101. Retrieved from https://link.aps.org/doi/10.1103/PhysRevLett.122.105101 doi: 10.1103/PhysRevLett.122.105101

Hurley, K., Dingus, B. L., Mukherjee, R., Sreekumar, P., Kouveliotou, C., Meegan, C., ... Niel, M. (1994, December). Detection of a γ-ray burst of very long duration and very high energy. *Nature*, *372*(6507), 652–654. Retrieved from https://doi.org/10.1038/372652a0 doi: 10.1038/372652a0

Koch, H. W., & Motz, J. W. (1959, Oct). Bremsstrahlung cross-section formulas and related data. *Rev. Mod. Phys.*, *31*, 920–955. Retrieved from https://link.aps.org/doi/10.1103/RevModPhys.31.920 doi: 10.1103/RevModPhys.31.920

Moss, G. D., Pasko, V. P., Liu, N., & Veronis, G. (2006). Monte Carlo model for analysis of thermal runaway electrons in streamer tips in transient luminous events and streamer zones of lightning leaders. *Journal of Geophysical Research: Space Physics*, *111*(A2), 1-37. Retrieved from https://agupubs.onlinelibrary.wiley.com/doi/abs/10.1029/2005JA011350 doi: 10.1029/2005JA011350

Nemiroff, R. J., Norris, J. P., Kouveliotou, C., Fishman, G. J., Meegan, C. A., & Paciesas, W. S. (1994, March). Gamma-Ray Bursts Are Time-asymmetric. *Astrophysical Journal*, *423*, 432-435. doi: 10.1086/173819

Norris, J. P., Nemiroff, R. J., Bonnell, J. T., Wickramasinghe, W. A. D. T., Kouveliotou, C., Paciesas, W. S., ... Meegan, C. A. (1994, November). Gross Spectral Differences between Bright and DIM Gamma-Ray Bursts. *Astrophysical Journal Letters*, *435*, L133. doi: 10.1086/187612

Pu, Y., Cummer, S. A., Lyu, F., Briggs, M., Mailyan, B., Stanbro, M., & Roberts, O. (2019, June). Low Frequency Radio Pulses Produced by Terrestrial Gamma-Ray Flashes. *Geophysical Research Letters*, *46*(12), 6990-6997. Retrieved from https://agupubs.onlinelibrary.wiley.com/doi/abs/10.1029/2019GL082743 doi: 10.1029/2019GL082743

Skeltved, A. B., Østgaard, N., Mezentsev, A., Lehtinen, N., & Carlson, B. (2017). Constraints to do realistic modeling of the electric field ahead of the tip of a lightning leader. *Journal of Geophysical Research: Atmospheres*, *122*(15), 8120-8134. Retrieved from https://agupubs.onlinelibrary.wiley.com/doi/abs/10.1002/2016JD026206 doi: 10.1002/2016JD026206

Xu, W., Celestin, S., & Pasko, V. P. (2015, January). Optical emissions associated with terrestrial gamma ray flashes. *Journal of Geophysical Research: Space Physics*, *120*(2), 1355-1370. Retrieved from https://agupubs.onlinelibrary.wiley.com/doi/abs/10.1002/2014JA020425 doi: 10.1002/2014JA020425

Xu, W., Celestin, S., Pasko, V. P., & Marshall, R. A. (2019, August). Compton Scattering Effects on the Spectral and Temporal Properties of Terrestrial Gamma-Ray Flashes. *Journal of Geophysical Research: Space Physics*, *124*(8), 7220-7230. Retrieved from https://agupubs.onlinelibrary.wiley.com/doi/abs/10.1029/2019JA026941 doi: 10.1029/2019JA026941

Østgaard, N., Neubert, T., Reglero, V., Ullaland, K., Yang, S., Genov, G., ... Al-nussirat, S. (2019, December). First 10 Months of TGF Observations by ASIM. *Journal of Geophysical Research: Atmospheres*, *124*(24), 14024-14036. Retrieved from https://agupubs.onlinelibrary.wiley.com/doi/abs/10.1029/2019JD031214 doi: 10.1029/2019JD031214